Studying Polymer-Dispersed Liquid-Crystal Formation by FTIR Spectroscopy. 2. Phase Separation and Ordering

Rohit Bhargava, Shi-Qing Wang, and Jack L. Koenig*

Department of Macromolecular Science, Case Western Reserve University, Cleveland, Ohio 44106

Received May 4, 1999; Revised Manuscript Received October 15, 1999

ABSTRACT: Polymerization-induced phase separation to form polymer-dispersed liquid crystals (PDLCs) is a complex process involving simultaneous curing and phase separation to form nematic microdomains. Real-time FTIR spectroscopy has been used to simultaneously observe and quantify the curing process using a model system—a fast photocurable matrix (NOA65) and a liquid crystal (E7). While the role of FTIR spectroscopy in monitoring chemical changes is well recognized and reinforced for PDLCs, it is demonstrated in this paper that it is also a powerful tool to monitor physical changes (phase separation and nematic ordering). Phase separation was detected during the curing process by a scattering-induced change in the absorbance spectrum of the sample. Nematic ordering could be observed and quantified based on a change in a characteristic band of the liquid crystal. Moreover, the phase separation and the onset of nematic ordering are temporally resolved. The conversion at phase separation decreases strongly with an increase in liquid-crystal content, while the conversion required for phase separation increases with increasing temperature. Isotropic droplets are formed followed by nematic ordering in the domains at lower E7 concentrations, while the processes are simultaneous for higher concentrations. Temperatures close to and above the LC transition temperature also lead to isotropic domains, which form nematic domains upon cooling. The fraction of liquid crystal present as nematic droplets and total fraction of nematic domains in the PDLC are quantified based on changes in the vibrational spectrum of E7. On the basis of mass balances applied to the closed process, the phase diagram of the system could be determined as a function of curing temperature. Solubility limits obtained by this method agree well with results obtained by other researchers. The concept of a spectroscopic composite plot that completely describes the formation process in a PDLC is proposed.

Introduction

Phase separation induced in a homogeneous mixture of prepolymer and liquid crystals by UV-initiated matrix polymerization is the current method of choice to produce PDLCs. The generally accepted picture is that as the matrix cures, it increases in molecular weight, specific interactions (if any) are lost, and its solubility parameter with the liquid-crystal changes. Phase separation is induced between the growing polymer and liquid crystal, causing small domains of liquid crystal to form. Domain growth is arrested by gelation with the cured and cross-linked matrix also imparting long-term stability to the formed structures. It has also been postulated that following initial liquid−liquid phase separation, further "purification" of the droplets takes place due to diffusion of the matrix material toward the boundary. This purification is hypothesized to be the trigger for nematic order to be attained in the droplets.[1] In another formulated theory of the phenomenon, cross-linking founded elastic forces have been postulated to affect the phase-separation process[2] resulting in liquid−gel demixing. The extent and structure of the polymer gel strongly influences the phase separation process and morphology evolution.[3] This, in turn, is shown to strongly influence performance properties of the PDLC.[4] In any case, it is clear that the interplay between photoinduced curing kinetics, phase separation, and nematic ordering is a complex series of interdependent formation events that have a controlling influence on the properties of the final product. New methods to reduce mutual solubility in the photoinduced phase separation process have recently been suggested.[5] They also require an investigation of the interplay between reaction kinetics and phase separation.

Experimental conditions strongly affect the photo-induced polymerization kinetics,[6] onset of phase separation vis-à-vis gelation and the dynamics of nematic ordering. These interdependent events not only are interesting phenomena but also determine the mutual solubility of the added components, morphology,[7] and electro-optical performance[8] of PDLC films.[9−11] Thus, a simple methodology to study these formation aspects with a view to relate them to performance properties is of scientific and commercial importance. In this paper, we present a simple method to study the phase-separation and ordering process while the cross-linking reactions are being observed using a rapid scan FTIR spectrometer.

Light scattering, polarized microscopy, and DSC (from changes in specific heat upon mixing)[12−14] have been used to obtain phase diagrams for uncured prepolymer/liquid-crystal mixtures. The curing kinetics of these mixtures have then been examined using photo-DSC by adjusting the temperature to be in the one-phase[14] and/or two-phase region.[13] DSC has also been used to examine the curing kinetics of some other polymer/nematic liquid-crystal systems.[15,16] The cured samples are then scanned across a temperature range, and the liquid-crystal phase separation is quantified based on transition enthalpies or glass transition changes. On the basis of these observations, solubility limits were obtained. Light-scattering and composition-dependent morphology studies can also yield solubility limits along with other information. However, they do not reveal any chemical information, and a second set of experiments is necessary to determine the chemical state of the film.

* Author to whom correspondence should be addressed.

10.1021/ma9907082 CCC: $18.00
Published on Web 12/03/1999

FTIR spectroscopy is an easily accessible, direct, and noninvasive method of examining chemical changes and has been applied to study PDLC formation.[17] Drawbacks in monitoring polymerization by using DSC were eliminated by using real-time FTIR spectroscopy to monitor the formation of such composites. However, for systems that do not have strong specific interactions between components, there is currently no methodology to detect other changes in the sample (e.g., phase separation) during the composite formation in an FTIR spectrometer. It is the aim of this paper to demonstrate the physical changes that can be monitored using the vibrational spectrum of the composite. This information is subsequently analyzed to yield important results about the phase-separation process, nematic ordering, and developed morphology.

Detecting Phase Separation, Nematic Ordering and Phase Compositions

Detecting Phase Separation Using FTIR Spectroscopy. The presence of an interface with a change in refractive index, as is the case with PDLCs, causes incident radiation to be scattered. Thus, if an initially homogeneous solution is cured leading to phase separation at some point, a sudden increase in scattering will be observed at that point of time. Monitoring this onset of turbidity or strong light scattering is usually the method of choice to examine the onset of phase separation.[18] Photo-DSC, incorporating a turbidity detection mechanism, has been used to simultaneously study curing and the onset of phase separation.[19] However, it was unclear if the scattering was a result of phase separation or nematic ordering as the two events were not resolved. Similarly, if a phase-separated sample were to be placed in the beam path of an infrared spectrometer, the transmitted intensity (of incident radiation on the sample) would be lower than the case where the same sample would have been homogeneous. The ratio of a single beam profile of such a scattering sample to the single beam profile of a background (no sample or homogeneous sample) would show this loss in intensity to be an absorbance in infrared absorbance spectra. This effect has been shown to result in an offset from the baseline in absorbance spectra.[20]

Thus, if a homogeneous mixture (as is a precursor for PDLC preparation) is cured, leading to phase separation, optical effects leading to baseline changes would be expected as a sign of the onset of phase separation. Conceptually, it is possible to simultaneously detect the onset of phase separation and curing reactions during PDLC formation by observing baseline and absorbance changes in real-time FTIR spectra. This type of method eliminates the need for specific interactions to observe changes in the miscibility of components. Phase separation may be detected in any system if the formed domain size is sufficient to scatter IR radiation. In this respect, it is a somewhat poorer method to detect phase separation compared to conventional light scattering. However, IR spectroscopy is a chemically specific probe and allows for detection of other (chemical and physical) processes at the same time.

Detection of Nematic Ordering Using FTIR. It has also been shown that the state of ordering in a liquid crystal is evident in its vibrational spectrum.[21,22] In particular, the absorbance of the nitrile stretching band from the liquid crystal considered here (E7) changes as the liquid crystal is brought into the nematic phase from an isotropic state. By monitoring these changes with time, it should be possible to detect the onset of nematic organization and, possibly, the dynamics of organization leading to quantification of the fraction of total liquid crystal that is nematic. For E7, only the liquid crystal in the nematic phase contributes positively to performance in a PDLC. It is then imperative to quantify the amount of liquid crystal in the nematic domains. The rest of the added liquid crystal is considered dissolved in the matrix and hence, wasted. On the basis of the absorbance of a liquid-crystal-specific band that shows a change (in our case, the nitrile stretching band of E7), it is possible to quantify the fraction of liquid crystal that manifests itself in nematic domains.

It is the objective of this paper to demonstrate that the onset of phase separation and nematic ordering can be monitored along with curing kinetics using real-time FTIR spectroscopy. These experimental observations are then analyzed to obtain information about the chemical and physical state of the composite. We use the NOA65−E7 system as a model system to demonstrate the utility of FTIR spectroscopy in monitoring aspects of PDLC formation at given experimental conditions in one single experiment. These results are then compared to results from DSC, microscopy and other FTIR experiments.

Expressions to Estimate Phase Composition. Let A_I be the absorbance of the liquid-crystal-specific band in its isotropic state and ϕ be the fraction of liquid crytsal (E7) in the initially homogeneous mixture with the matrix precursor (NOA65). Then, correcting for a constant cell thickness, the absorbance of the liquid-crystal-specific band (here the absorbance due to CN stretching vibration) is simply

$$A_{CN,uncured} = \phi A_I \tag{1}$$

If α is the fraction of liquid crystal that phase separates, then the total fraction of the liquid crystal in the droplets is $\alpha\phi$ and the overall absorbance of the liquid-crystal-specific band is

$$A_{CN,cured} = A_N \alpha\phi + A_I \phi(1 - \alpha) \tag{2}$$

Rearranging the two equations to eliminate ϕ

$$\alpha = \left(\frac{A_{CN,uncured} - A_{CN,cured}}{A_{CN,uncured}}\right)\left(\frac{A_I - A_N}{A_I}\right)^{-1} \tag{3}$$

or

$$\alpha = \left(\frac{\Delta A_{CN,curing}}{A_{CN,uncured}}\right)\left(\frac{A_I}{\Delta A_{I\rightarrow N}}\right) \tag{4}$$

Thus, the fraction of liquid crystal in nematic domains is simply the ratio of the fractional change in absorbance of a band on curing with the fractional change in absorbance due to the isotropic to nematic transition. The assumption of constant cell thickness is redundant as is the dependence on ϕ. Preferential dissolution of components and the loss of specific interactions with the matrix that may affect absorbance are assumed to be small and are neglected.

The solubility of liquid crystal in the matrix (especially for the NOA65/E7 system) has been examined experimentally by DSC, FTIR mapping,[23,24] and FTIR imaging[5] and indirectly by the construction of phase diagrams from microscopy observations.[7] In the case

here, the fraction of liquid crystal that is nematic allows for the determination of solubility limits. Clearly the maximum concentration of liquid crystal that does not phase separate on curing is the solubility limit of the liquid crystal in the matrix at that temperature and conversion. Thus, if α is plotted against ϕ, the solubility limit can be determined by the intersection of the curve with the x axis. This minimum concentration required for droplet formation is denoted by Φ_{LC}. Assuming that we are dealing with a phase-separated system, the amount of matrix material dissolved in the nematic liquid-crystal domains can also be determined as follows.

If a unit mass of liquid crystal−polymer composite is considered, then the fractional mass in nematic domains due solely to liquid crystal is given by

$$x_L = \alpha\phi \tag{5}$$

and the total material in nematic domains can be obtained as $(x_L + x_M)$, where x_M is the fractional mass of matrix material dissolved in the nematic domains. Similarly, if the fractional mass of liquid crystal in an isotropic state (dissolved in the matrix) is y_L and the fractional mass of matrix material (in the isotropic matrix) is y_M, then mass balances yield

$$x_L + y_L = \phi \tag{6a}$$

$$x_M + y_M = 1 - \phi \tag{6b}$$

The fraction of liquid crystal dissolved in the matrix (isotropic) can be given by

$$\frac{y_L}{y_L + y_M} = \Phi_{LC} \tag{7a}$$

Similarly, the fraction of matrix material in a nematic domain can be given by

$$\frac{x_M}{x_L + x_M} = \Phi_M \tag{7b}$$

Equations 5−7 are a system of five equations with five variables. The starting composition (ϕ) and fraction of liquid crystal (α) separated into nematic domains are known from the IR experiment. A plot of α against ϕ gives the limiting value Φ_{LC}. Hence, ϕ_M can be expressed in terms of α, ϕ, and Φ_{LC} as

$$\Phi_M = \frac{\Phi_{LC}(1 - \alpha\phi) - \phi(1 - \alpha)}{\Phi_{LC} - \phi(1 - \alpha)} \tag{8}$$

where it is implicit in the derivation that the systems are phase separated, i.e., $\alpha > 0$. Using eqs 4 and 8, it is possible to construct a "phase-diagram" for the system based on its curing temperature. Once cross-linked, the matrix is almost impermeable to the liquid crystal, and hence, one cannot carry out the classical one-phase to two-phase transition by a small change in temperature. Hence, in the true sense of the term, the plot discussed is a pseudo phase diagram. This plot is useful in giving the intercomponent solubility limits and state of organization of the liquid crystal for a curing temperature. From the proposed data examination techniques above, it appears possible to use FTIR spectroscopy to examine the important events and quantities for PDLC formation during the formation process.

Experimental Section

Materials. The low molecular weight liquid crystal used in this study is a liquid-crystal mixture, E7.[25] The nematic−isotropic transition temperature of this system is reported to be about 330 K with a glass transition temperature of about 210 K. The polymeric matrix, NOA65, is reportedly a UV-curable prepolymer mixture composed primarily of trimethylolpropane diallyl ether, trimethylolpropane tris(thiol), isophorone diisocyanate ester, and a benzophenone photoinitiator.[13] All materials were used as received. A second confirmatory set of experiments was done with a different batch of materials obtained from the same sources.

Sample Preparation. Mixtures by weight of LC and NOA65 were used to prepare the samples. The mixture was weighed, hand mixed for 2 min, and heated to 70 °C (well above the clearing point of E7) and mixed again. Samples were cast directly onto a NaCl salt plate containing 10 μm diameter spacers on the edges and sandwiched by another salt plate. The sandwiched assembly was subjected to a constant weight for 15 min to apply pressure in order for it to attain hydrodynamic equilibrium. Constant spacing between the substrates was assured by sandwiching the salt plates between two metal apertures fixed in round brass plates. This assembly was screwed together and inserted into a heating jacket that also serves as a sample holder. Metal apertures on either side of the salt plate were used for three reasons. They allow the region probed by the IR beam to be away from the boundary (where the spacers were used) and thus free of any boundary effects or influences due to the presence of spacers.

The small apertured region was examined before curing using an Olympus Stereo microscope with a 15× magnification to ensure that there were no air bubbles or spacers present in the regions examined. Aperturing also allows the examined material to be surrounded by uncured low viscous material in two dimensions, thus relieving contraction-induced stress.[26] Sample thickness was kept constant with a variation of less than 5% from sample to sample. The mounted sample was subjected to UV radiation at a wavelength of 365 nm obtained using a hand-held UV lamp[27] incorporated into the spectrometer at a fixed position. Thus, the intensity of the UV radiation was held constant for all experiments. Measured intensity of incident UV radiation at the surface of the sample was 1 mW/cm^2 measured using a Series 9811 Radiometer[28] whose least count was 0.01 mW/cm^2. The lamp was allowed to equilibrate for at least a half hour before any experiments were conducted. Temperature was controlled in the custom-built sample holder by using an Omega CN 5000[29] proportional temperature controller. The temperature was also independently measured at a point diametrically across from the measurement for the controller using an Omega HH21 thermocouple based thermometer. Maximum fluctuation in temperature decreased from about ±0.8 K at 300 K to about ±0.2 K at 335 K.

Instrumentation. The FTIR spectrometer used in this study was the Bio-Rad FTS 6000 incorporating an MCT detector.[30] A nominal spectral resolution of 4 cm^{-1} over the mid-infrared range and a time resolution of 0.935 s were used for kinetic studies. This time resolution was deemed sufficiently small to capture the essence of the curing reaction while allowing satisfactorily high signal-to-noise ratio spectra. Five scans were co-added for each data point.

Results and Discussion

Phase Separation During Curing. Figure 1a shows the curing reaction progression of a phase-separating composition (50% E7 cured at 300 K) and their corresponding difference spectra for various times as indicated (Figure 1b). No scattering occurs for a homogeneous mixture while strong scattering (due to nematic phase-separated domains) occurs at a higher conversion. A small offset in the baseline signals the onset of phase

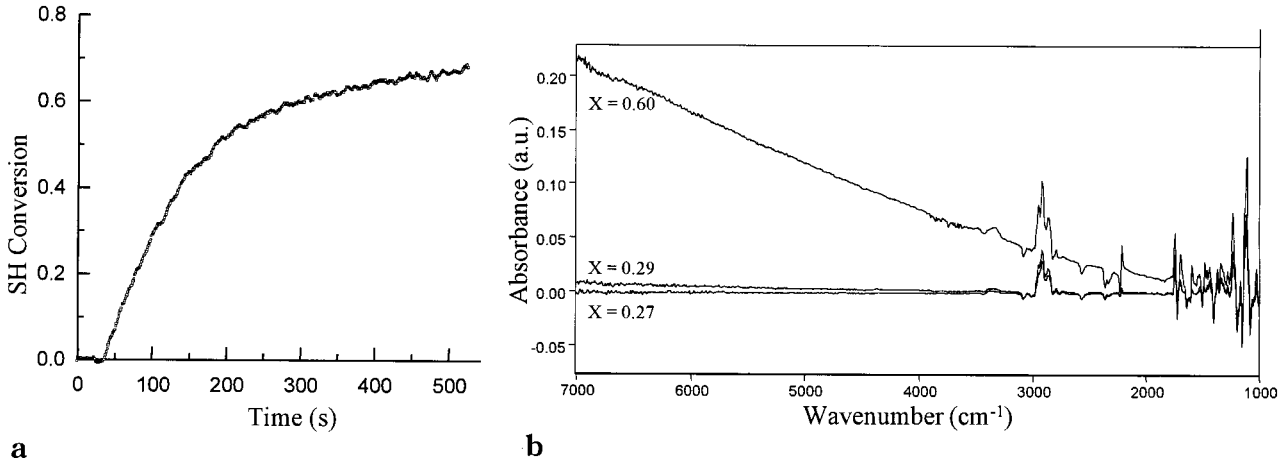

Figure 1. (a) Conversion vs time plot for a phase separating mixture and (b) the corresponding difference spectra at various conversions. Phase separation occurs at $X \sim 0.28$ for the 50% E7 mixture (shown above) cured at 300 K.

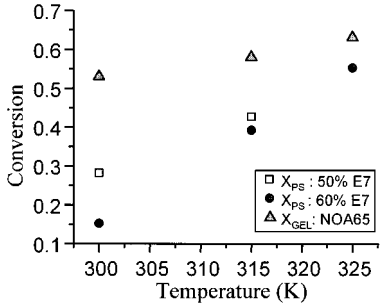

Figure 2. Temperature dependence of the conversion at phase separation for two E7 concentrations in NOA65.

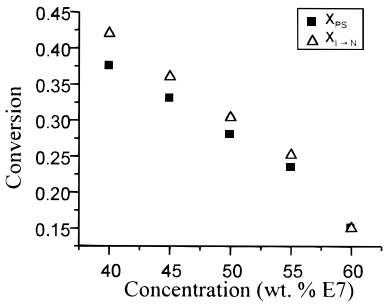

Figure 3. Conversion at the onset of phase separation and at the onset of nematic ordering for phase-separating mixtures examined at 300 K.

separation. The minimum conversion that results in an offset sufficiently above the noise levels is compared to the highest conversion at which the baseline is unambiguously straight (as shown for conversions of 0.27 and 0.29 in Figure 1b). An average of the two values is taken to be the conversion at the onset of phase separation. Using data from plots such as Figure 1, the conversion at the onset of phase separation is determined. Results are shown for two liquid-crystal concentrations phase separating at different temperatures (Figure 2).

The conversion at gelation can be deduced from curing kinetics. This conversion is characterized as the time at which the rate of reaction is considerably slowed due to the increased viscosity of the gel. From a plot of the rate of reaction against conversion,[6] the conversion at the gel point may be deduced. The conversion at gelation is of practical importance as this is the one singular event that influences the development of phase separated structures. For thiolene systems, the Flory–Stockmayer theory was found to adequately predict the conversion at gelation, x_{gel}.[31,32] It is difficult to obtain the gel point of a phase-separating mixture that has some solubility of the matrix in the liquid crystal as the reaction is now in two phases with very different kinetic behaviors. Moreover, the reaction of the matrix material in liquid-crystalline domains persists even after gelation has set in for the liquid-crystal-poor regions.[33] A convenient reference point is the conversion where the reaction has considerably slowed. This is indicated as the gel point for the composite and can be seen to be almost constant.

The conversion required for phase separation increases progressively with increasing temperature and is superseded by gelation at some point (e.g., at 335 K for the 50% E7) leading to a homogeneous film. Among the concentrations examined, phase separation is seen for concentrations greater than 30% at 300 K (Figure 3). Phase separation occurs early in the curing process for many cases. As the liquid-crystal content is increased, conversion required for phase separation decreases. Caution needs to be exercised here as the observation of no scattering may not imply that the material is homogeneous in some cases.[34] Those aspects are considered and further results are derived from trends as shown here. The trends are probably more reliable compared to a single observation of scattering and observed values would at least correspond well with upper bounds to the solubility at a given temperature.

Detection of Nematic Order During Curing. The decrease in the absorbance of the nitrile band absorbance signifies the onset and progression of nematic ordering. The onset of nematic ordering in reference to the onset of phase separation and neat NOA65 gelation is shown in Figure 3. It can be seen that there is a significant lag in the onset of nematic ordering for lower concentrations while it is simultaneous for the higher concentrations. This points to difference in mechanism of phase separation for the two concentrations. The lower concentration probably proceeds through liquid–gel decomposition[3] with the polymer being involved as microgel particles or is due to a significant solubility of the oligomers. This is also supported by the conversion of the SH group for 40% and 45% LC at 300 K being somewhat higher than the other phase-separated concentrations.[6] The higher concentrations, esp. 60% LC content, are probably a result of liquid–liquid decomposition given the co-incidence of phase separation and ordering onset.[3] Samples at higher temperatures were

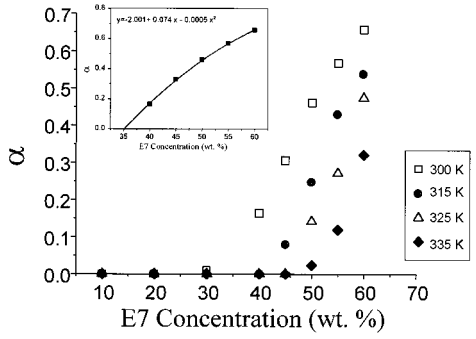

Figure 4. α values obtained for different temperatures as a function of E7 concentration. The inset shows the trend in values at 300 K. The fitted curve yields the point of intersection with the *x* axis to be 35.1%.

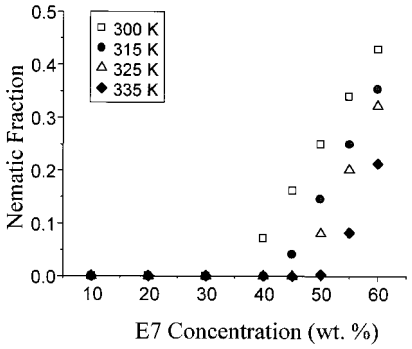

Figure 5. Mass fraction of nematic domains in a PDLC as a function of E7 concentration at different temperatures.

all cooled back to 300 K, and α was calculated. The ones that were isotropic at the curing temperature showed a jump in values.

It is pertinent to point out that, due to infrared wavelength limitations, the scattering evidenced in the baseline shifts that we consider the onset of phase separation is probably manifested at a later time than phase separation has occurred or even that would be detected using other scattering techniques. The onset of nematic ordering is molecular level information that IR spectroscopy would pick up almost instantaneously after occurrence. Thus, the difference between the onset of phase separation and nematic ordering that we see may actually be larger. Keeping that in mind, the conclusion of liquid−gel demixing as a decomposition mode is probably true for lower E7 concentrations. At the same time, the phase-separated structures for 60% E7 concentration would develop much quicker than 40% while the rate of reaction is lower. Thus, the difference in conversion that is detected is probably much less in error than that for 40%. Hence, it is conceivable that the 60% E7 concentration undergoes liquid−liquid demixing. On the basis of the differences seen in the small (20%) range in composition, it may be concluded that the mode of phase separation is very sensitive to liquid-crystal concentration in such systems. It may also be conceived that the morphology at 40% LC content is probably farther from spherical than phase separation for 60% LC. Later phase separation leading to this type of effect has been evidenced in another system. Thus, a measurement (using FTIR) considered highly chemical specific in nature also gives clues to the physical state of development in systems such as the one studied here.

A faster rate at higher temperatures implies that the systems reach their gel point more quickly. Coupled with higher thermodynamically dictated solubility at higher temperatures, the fraction of liquid crystal remaining dissolved in the matrix increases sharply with temperature. Following eq 4, α values are obtained for the mixtures at 300 K after 20 min of curing. Small (typically on the order of 0.01−0.05) α values are seen for smaller concentrations followed by a jump in values, which then increase steadily with concentration. The small positive values at lower concentration are probably a result of the liquid crystal confined to the free volume created by polymerization and/or by loss of specific interactions with the matrix. When the trends from those small values are subtracted from the obtained α values, corrected α values are obtained, and these are used in our calculations. Trends can be seen in Figure 4. The maximum concentration of liquid crystal that does not appear as droplets is considered to be the solubility of liquid crystal at that temperature. A fitted curve to corrected α values gives the solubility limit as shown in the inset in Figure 4. Limiting values are obtained by setting $y = 0$ in the equation of the curve.

Using these α and $\Phi_{LC,\,M}$ values, eqs 5−7 are solved for the unknown quantities. The fraction of PDLC that is in the nematic phase is then $(x_L + x_M)$. This fraction is plotted as a function of liquid-crystal concentration at different temperatures in Figure 5. The values are only marginally higher than the ones obtained by considering the solubility to be just x_L. The correction is a maximum of about 5%. These values subtracted from 1 obviously give the fraction in the nonnematic phase. In excellent agreement with the DSC results of Smith, it can be seen that only about half of the liquid crystal added (at 300 K for a 50:50 starting composition) is phase separated. This type of plot is a ready reference that shows the fraction of liquid crystal in the PDLC as a function of the liquid crystal added to the initial mixture.

The fraction of the nematic phase that is the matrix material is x_M. Its value does not change much over the temperature range examined with the range being 8−12%. NOA65 in the nematic phase is as low as 4% at 255 K.[5] Hence, E7 domains with concentrations of NOA65 below about 5% are nematic until the T_{NI} is reached. Nematic droplets are obtained for most of the region below the coexistence curve. There is a small region above about 330 K, where the nematic ordering could only be discerned by cooling the sample. That is probably due to the droplets being isotropic and the region is labeled as such. The other regions in the temperature−composition space yield only a single-phase film. These observations can be plotted on a phase diagram as discussed in the Introduction section and shown in Figure 6. $\Phi_{LC,M}$ and $\Phi_{M,LC}$ can be used to estimate the phase compositions formed at each temperature. They are the points where a tie line at a particular temperature would intersect the coexistence curve. The curves are drawn as best fit to act as an aid to the eye. In principle, more experiments could be conducted at different temperatures and the curves determined more accurately. However, the example shown above illustrates an important application of FTIR and the extent of information that can be derived from a very small set of experiments.

Mutual Solubility of Liquid Crystal and the Matrix. Solubility issues in the E7/NOA65 system have been examined by other researchers using optical microscopy,[7] DSC, FTIR mapping coupled with micros-

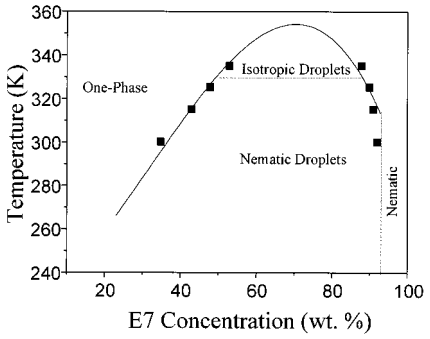

Figure 6. Phase diagram of E7/NOA65 based on vibrational spectroscopic observations.

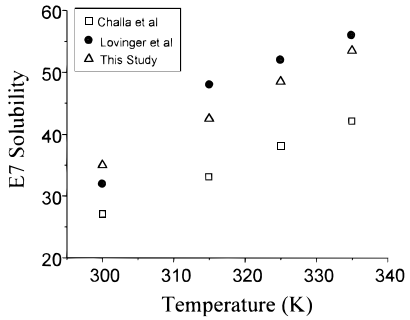

Figure 7. Solubility limits of E7 in NOA65 as a function of temperature. Results are compared with similar studies by other researchers.

copy,[23,24] and FTIR Imaging.[5] Two studies have suggested E7 solubility in the matrix over a range of temperature. Results from those two are compared with results obtained by our method in Figure 7. The trends from each are very similar to the values differing by less than ±7% in most cases, which can be said to be in excellent agreement as the magnitude of error was ~±3% in the reported measurements. As expected, the solubility increases with an increase in temperature. We have also deduced the solubility of the matrix material in the liquid crystal. The solubility is approximately 10% with a deviation of ±2% across the temperature range examined.

The relative invariance of the matrix solubility is a surprising result caused probably by the uniqueness of this form of phase separation induced by cross-linking. At higher temperatures, the matrix material not only reacts faster but also reacts to a higher conversion. Coupled with phase separation late in the curing process, most of the matrix material is polymerized at the time of the onset of phase separation. The size of each (un-cross-linked) potentially dissolvable molecule is larger. Hence, compared to lower temperatures dissolution is hindered by both thermodynamic and kinetic considerations. This partly offsets the expected higher solubility at higher temperature and explains the result seen. It is to be pointed out that an FTIR investigation only gives the number of nitrile groups that are in the nematic phase, i.e., the number of liquid-crystal molecules that are phase separated. As in this study, liquid-crystal mixtures are typically used in actual applications to extend the thermally allowable operational range of the device. We have assumed that each molecule corresponds to a certain mass and, hence, gives a direct relation between the number and mass of both matrix and liquid-crystal molecules. This assumption of a pseudobinary system may introduce some error in the results as components of these mixtures may phase

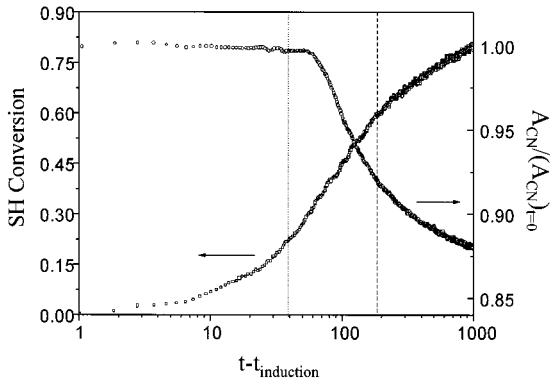

Figure 8. Composite plot for PDLC formation shown for a 40% E7 mixture at 300 K. The first vertical line denotes the onset of phase separation while the one on the right denotes matrix gelation.

separate at different rates. This would lead to the relative composition of the liquid crystal or matrix material in the phases being different from the composition before the prepolymer and LC are mixed.[35] This is a phenomenon that cannot be examined using the technique outlined above but can be readily examined using FTIR imaging.[36]

A composite data plot of the type as shown in Figure 8 completely characterizes the formation of PDLCs at a given experimental condition. The conversion of reacting groups (in this case SH stretching) elucidates the chemical kinetics. A straight line parallel to the *y* axis, as deduced from baseline changes in difference spectra, indicates the onset of phase separation. The absorbance of a liquid-crystal-specific band (in this case the nitrile group stretching) gives the dynamics of liquid-crystal ordering, while the total fractional decrease in its absorbance gives a measure of the fraction of liquid crystal added that is present in nematic domains. From a series of such plots at different temperatures, all results discussed in this paper can be deduced.

Conclusions

Rapid scan FTIR spectroscopy was used to observe physical changes in a PDLC film based on its vibrational spectrum. Phase separation in PDLC forming precursors is detected in real time and temporally resolved from nematic ordering. It is shown that the processes are distinct in some cases and simultaneous in others depending on the fraction of liquid crystal added. The extent of nematic ordering in the PDLC was estimated by the change in a characteristic peak. This was related to the mutual solubility of the matrix material and liquid crystal. Applying mass balances, the composition of each phase was determined. This allows for the construction of phase diagrams based on the curing temperature. While the solubility of liquid crystal increased sharply with temperature, the matrix solubility was almost constant.

Relating this information to desired electrooptical properties would allow for faster optimization of experimental parameters to form PDLCs. Examining the curing kinetics and final conversion would give an indication of the long-term stability of the formed structures. That aspect affecting PDLC properties was easily examined using FTIR spectrometry. Additionally, we have obtained information about the phase separation process, hitherto not examined using FTIR, in the same experiment. The composition of the matrix and

the droplets was also determined. This is an important parameter in predicting the electrooptical properties and performance of the formed PDLC. The temporal resolution of phase separation and onset of nematic ordering allows for a guess at the mechanism of phase separation and the most probable morphology. Determining optimal conditions for curing to form PDLCs is a cumbersome trial-and-error process as the number of parameters affecting final properties is very large. Using the techniques outlined in this paper, much more information about the formation processes can be obtained from a single experiment and in a much smaller time period than was previously possible. A general methodology that simultaneously examines curing reactions, phase separation and organization in real time for polymer composite formation has been outlined. This may be usefully extended to other phase separating systems.

Acknowledgment. Funding for the project was provided by the National Science Foundation Center for Advanced Liquid Crystalline Optical Materials (ALCOM).

References and Notes

(1) Doane, J. W. In *Liquid Crystals, Applications and Uses*; Bahadur, B., Ed.; World Scientific: Singapore, 1990; Chapter 14, p 361.
(2) Boots, H. M. J.; Kloosterboer, J. G.; Serbutoviez, C.; Touwslager, F. J. *Macromolecules* **1996**, *29*, 7683.
(3) Serbutoviez, C.; Kloosterboer, J. G.; Boots, H. M. J.; Touwslager, F. J. *Macromolecules* **1996**, *29*, 7690.
(4) Serbutoviez, C.; Kloosterboer, J. G.; Boots, H. M. J.; Paulissen, F. A. M. A.; Touwslager F. J. *Liq. Cryst.* **1997**, *22*, 145.
(5) Bhargava, R.; Wang, S.-Q.; Koenig, J. L. *Macromolecules* **1999**, *32*, 2748.
(6) Part 1: Bhargava, R.; Wang, S.-Q.; Koenig, J. L. *Macromolecules* **1999**, *33*, 8982.
(7) Lovinger, A. J.; Amundson, K. R.; Davis, D. D. *Chem. Mater.* **1994**, *6*, 1726.
(8) Nazarenko, V. G.; Sarala, S.; Madhusudana, N. V. *Jpn. J. Appl. Phys., Part 1* **1994**, *5A*, 2641.
(9) Yamagishi, F. G.; Miller, L. J.; van Ast, I. C. *Liquid Crystals Chemistry, Physics and Applications*; Proccedings of SPIE-The International Society for Optical Engineering No. 1080; SPIE: Bellingham, WA, 1989; 1989, p 24.
(10) Legrange, J. D.; Carter, S. A.; Fuentes, M.; Boo, J.; Freeny, A. E.; Cleveland, W.; Miller, T. M. *J. Appl. Phys.* **1997**, *81*, 5984.
(11) Carter, S. A.; Legrange, J. D.; White, W.; Boo, J.; Wiltzius, P. *J. Appl. Phys.* **1997**, *81*, 5984.
(12) Smith G. W. *Phys. Rev. Lett.* **1993**, *70*, 198.
(13) Nwabunma, D.; Kim, K. J.; Lin, Y.; Chien, L. C.; Kyu, T. *Macromolecules* **1998**, *31*, 6806.
(14) Smith, G. W. *Mol. Cryst. Liq. Cryst.* **1994**, *239*, 63.
(15) Smith, G. W. *Mol. Cryst. Liq. Cryst.* **1994**, *241*, 77.
(16) Roussel, F.; Buisine, J.-M. *Liq. Cryst.* **1998**, *24*, 555.
(17) See the first part in this series by the same authors.[6]
(18) Smith, G. W.; Vaz, N. A. *Mol. Cryst. Liq. Cryst.* **1993**, *237*, 243.
(19) Kloosterboer, J. G.; Serbutoviez, C.; Touwslager, F. J. *Polymer* **1996**, *37*, 5937.
(20) Bhargava, R.; Wang, S.-Q.; Koenig, J. L. *Appl. Spectrosc.* **1998**, *52*, 323.
(21) McFarland, C. A.; Koenig, J. L.; West, J. *Appl. Spectrosc.* **1993**, *47*, 598.
(22) Bhargava, R.; Wang, S.-Q.; Koenig J. L. Manuscript under preparation.
(23) Challa, S. R.; Wang, S.-Q.; Koenig, J. L. *Appl. Spectrosc.* **1997**, *51*, 297.
(24) Challa, S. R.; Wang, S.-Q.; Koenig, J. L. *Appl. Spectrosc.* **1997**, *51*, 10.
(25) EM Industries, Inc., 7, Skyline Drive, Hawthorne, NY 10532.
(26) Tran-Cong, Q.; Harada, A. *Phys. Rev. Lett.* **1996**, *76*, 1162.
(27) UVP Inc., San Gabriel, CA 91778.
(28) Cole-Parmer Instrument Company, Chicago, IL 60648.
(29) Omega Engineering Inc., One Omega Drive, Box 4047, Stamford, CT 06907−0047.
(30) Bio-Rad Laboratories, Digilab Division, 237 Putnam Avenue, Cambridge, MA 02139.
(31) Chiou, B.-S.; Khan, S. A. *Macromolecules* **1997**, *30*, 7322.
(32) Chiou, B.-S.; English, R. J.; Khan, S. A. *Macromolecules* **1996**, *29*, 5368.
(33) West, J. L. *Mol. Cryst. Liq. Cryst. Inc. Nonlin. Opt.* **1988**, *157*, 427.
(34) For example, see discussions In Zumer, S.; Doane, J. W. *Phys. Rev.* **1988**, A34, 3373 and Montgomery, G. P., Jr.; Vaz, N. A. *Phys. Rev.* **1989**, A40, 6580.
(35) Nolan, P.; Tillin, M.; Coates, D. *Mol. Cryst. Liq. Cryst. Lett.* **1992**, *8*, 129.
(36) Bhargava, R.; Wang, S.-Q.; Koenig J. L. Manuscript under preparation.

MA9907082